TRACE-P OH and HO_2 measurements with the Airborne Tropospheric Hydrogen Oxides Sensor (ATHOS) on the DC-8.

NASA grant: NCC-1-414

Principal Investigator: William H. Brune
Co-Investigators: Monica Martinez-Harder, Hartwig Harder
(now at Max Planck Institute for Chemistry, Mainz, Germany)

Address: Department of Meteorology
503 Walker Building
Pennsylvania State University
University Park, PA

Introduction.

The Airborne Tropospheric Hydrogen Oxides Sensor (ATHOS) measures OH and HO_2 from the NASA DC-8. This instrument detects OH by laser induced fluorescence (LIF) in detection chambers at low pressure and detects HO_2 by chemical conversion with NO followed by LIF detection. The demonstrated detection limit (S/N=2, 5 min.) for OH is about 0.005 pptv ($1x10^5$ cm^{-3} at 2 km altitude) and for HO_2 is 0.05 pptv ($1x10^6$ cm^{-3} at 2 km altitude). We will use ATHOS to measure OH, HO_2, and HO_2/OH during TRACE-P, analyze these results by comparing them against fundamental relationships and computer models, and publish the analyses. TRACE-P HO_x measurements will help develop a clearer picture of the atmospheric oxidation and O_3 production that occur as Asian pollution spreads across the Pacific Ocean.

Besides contributing to the science goals outlined in the TRACE-P NRA, HO_x measurements could be combined with simultaneous measurements of environmental factors and other chemical species to test the following hypotheses:

- Asian outflow contains a unique mixture of HO_x sources; these, in combination with outflow and lightning NO_x, can shift large regions of the Pacific troposphere from being ozone-destroying toward being ozone producing;
- As Asian outflow mixes with cleaner Pacific air, ozone production that is calculated from HO_2 and NO measurements is greater than that calculated by chemical transport models;
- Atmospheric oxidation over the western tropical Pacific is affected by the evolution of Asian outflow, but whether it is increased or decreased depends on the composition of the outflow and the influence of convection on that composition.
- Asian aerosols influence HO_x and atmospheric oxidation; they must be considered when calculating the influence of the Asian outflow on the photochemistry of the Pacific troposphere.
- The outflow of HO_x sources into the Pacific free troposphere has greater influence on increasing ozone production than does the NO_x outflow because of the greater

horizontal range of HO_x sources compared to that of NO_x and the availability of NO_x from lightning.

Testing these hypotheses relies heavily on the simultaneous measurements of HO_x, all the chemical species that interact with HO_x, and the environmental conditions, particularly the photolysis frequencies. It is important to obtain this entire measurement suite from the planetary boundary layer to the ceiling of the DC-8 at 12 km, as well as in the presence of clouds and heavy pollution nearer the Asian coast. Measurements while flying out of and into airports are important photochemical kinetics tests because of the different amounts of NO that are mixed into the continental air. In addition, measurements must be made at different times of the day and night. All of these conditions were encountered during the TRACE-P study.

Results

ATHOS measured OH and HO_2 with good sensitivity on all flights. Data coverage was 89% for OH and 88% for HO_2.

Observations

The observations can be summarized as average values as a function of altitude and a few critical controlling variables. To put the TRACE-P measurements into context, they are plotted along with ATHOS measurements from SONEX and from PEM Tropics B. SONEX was in a different season (October-November) in 1997(Faloona et al., *J. Geophys. Res.*, **105**, 3771-3783); it was conducted at mid to high latitudes over the North Atlantic. Conditions were typically moderately polluted. PEM Tropics B was conducted over the relatively clean tropical Pacific in the same season as TRACE-P (March-April) in 1998 (Tan et al., *J. Geophys. Res.*, **106**, 32,667). The results of these two studies provide a good contrast with TRACE-P, which was over the mid latitude eastern Pacific in the Asian continental outflow.

As a function of altitude in TRACE-P, OH is a constant 0.1 pptv up to 8 km, where it then increases to 0.2 pptv by 11 km (Figure 1a). HO_2 on the other hand increases from 10 pptv near the surface to 12.5 pptv at 2-4 km, just above the marine boundary layer, before monotonically decreasing to 7 pptv at 11 km (Figure 1b). Interestingly the behavior of OH in TRACE-P is similar to OH in SONEX, while HO_2 in TRACE-P behaves more like HO_2 in PEM Tropics B.

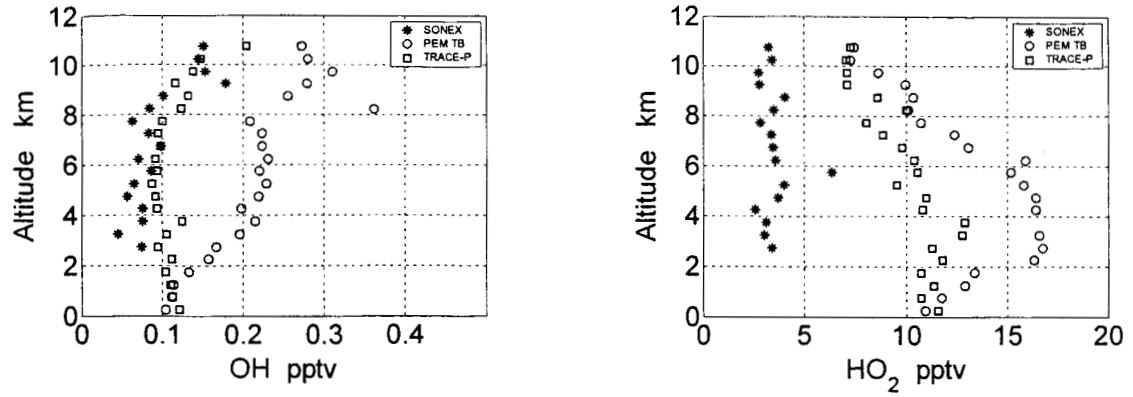

Figure 1. Altitude profile of HO_x for TRACE-P, SONEX, and PEM Tropics B. The mean daytime (SZA<80°) profiles are given for (a) OH and (b) HO_2.

OH and HO_2 depend critically on a few controlling variables. Perhaps the most important among these are NO and the production of HO_x. We examine each in order.

We expect that OH will initially increase as a function of NO, since NO reacts with HO_2 and shifts the balance of OH and HO_2 towards OH. HO_2, on the other hand, will be initially independent of NO, but will then decrease as a function of NO as $HO_2+NO \rightarrow OH+NO_2$ shifts HO_2 toward OH and $OH+HO_2 \rightarrow H_2O+O_2$, a fast reaction, becomes the dominant sink for HO_x. Indeed, these behaviors are observed. Once again, OH in TRACE-P is similar to OH in SONEX, while HO_2 in TRACE-P is similar to HO_2 in PEM Tropics B.

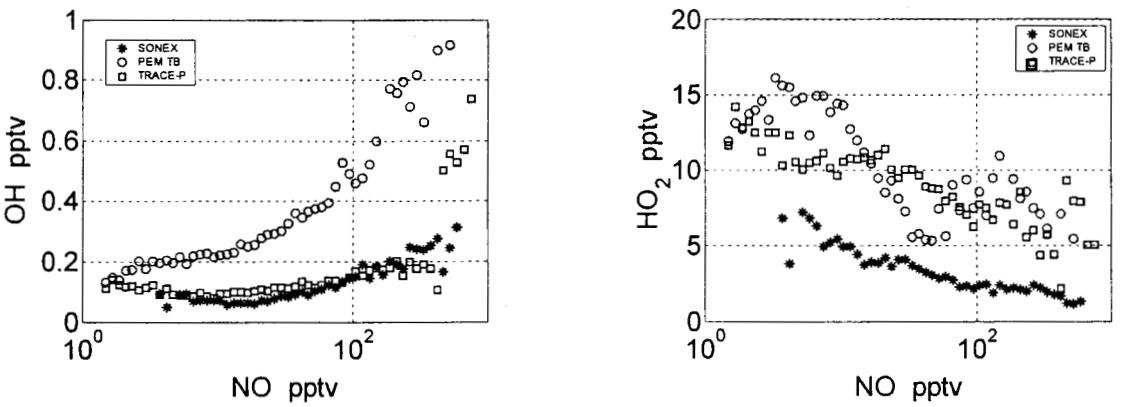

Figure 2. Mean HO_x as a function of NO for TRACE-P, SONEX, and PEM Tropics B. The mean daytime values are given for (a) OH and (b) HO_2.

Since the predominant HO_x source in all these studies is calculated to be the photolysis of ozone followed by the reaction of $O(^1D)$ with H_2O to form OH, the second controlling variable we chose is the photolysis frequency for $O_3+h\nu \rightarrow O_2+O(^1D)$. Simple atmospheric chemistry theory suggests that the slopes of these lines should be approximately ½, while the observed slope for OH and HO_2 in TRACE-P is closer to ⅓. The slope is similar to that observed in PEM Tropics B, but is less than the slope in

SONEX, which is very close to ½. The observed and modeled values are compared in a following section.

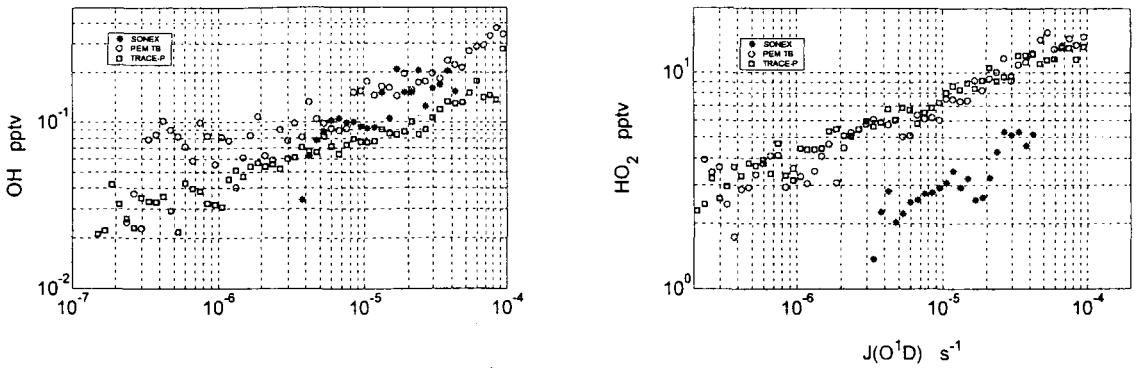

Figure 3. Mean HO_x as a function of $J(O(^1D))$ for TRACE-P, SONEX, and PEM Tropics B. The mean daytime values are given for (a) OH and (b) HO_2.

The ratio of HO_2 to OH is a sensitive indicator of the sum of reactions of OH with CO and volatile organic compounds (VOCs) to produce HO_2 and the reaction of HO_2 with NO and to a lesser extent O_3 to form OH. Because HO_2 decreases with increasing NO while OH first rises and then decreases at a slower rate than HO_2 with NO, the HO_2/OH ratio is expected to decrease with increasing NO. The observed HO_2/OH ratio does (Figure 4.) That the HO_2OH ratio is much greater for TRACE-P than for either SONEX or PEM Tropics B suggests that the air sampled during TRACE-P contained much more CO and VOCs than the air encountered during either SONEX or PEM Tropics B.

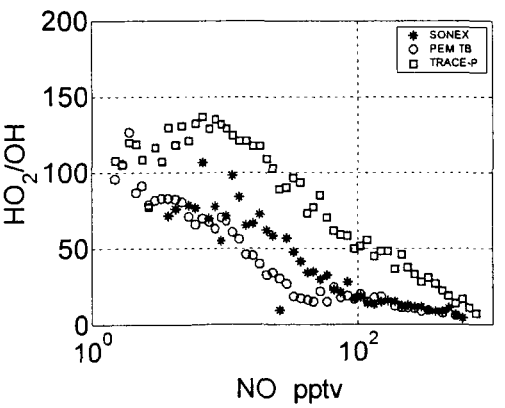

Figure 4. Mean HO_2/OH versus NO for TRACE-P, SONEX, and PEM Tropics B.

Comparison to other HO_x instruments.

It is essential to compare the measurements of the same chemical species by different instruments on different aircraft. Such comparisons must be part of every field deployment if the different aircraft are to function as one. Quite good comparisons were arranged between the NASA DC-8 and the NASA P-3 and briefly between the NASA P-

3 and the NCAR C-130 during TRACE-P. The results of the comparison between measurements on the NASA DC-8 and NASA P-3B are documented in the paper by Eisele et al. (Eisele F. L., et al., Summary of measurement intercomparisons during TRACE-P, J. Geophys. Res., 108 (D20), 8791, doi:10.1029/2002JD003167, 2003) For OH, the slope of the NCAR CISIMS OH as a function of the DC-8 ATHOS OH is 1.5 with R^2=0.88, which is within the combined uncertainties of CISIMS (±60%) and ATHOS (±40%). This difference suggests a difference in the absolute calibration. Interestingly, during the second comparison, which occurred at an altitude of 5 km, the two measurements are within 20% of each other, suggesting a variable calibration of one or both instruments. For HO_2, only HO_2+RO_2 was measured by Cantrell and coworkers on the P-3B, and the slope of the NCAR PerCIMS HO_2+RO_2 as a function of the ATHOS HO_2 is 2.46 with R^2=0.78. Since model results suggest that HO_2 is approximately ½ of HO_2+RO_2, the ATHOS HO_2 measurements appear to be somewhat lower than what the NCAR PerCIMS HO_2+RO_2 suggests.

After these results became clear, we spent a considerable amount of time reviewing our calibrations and calibration procedures. The calibration light sources are now calibrated much more frequently and by at least three different methods. Just prior to TRACE-P, we greatly improved our detection sensitivity and in the process caused a change in the ATHOS calibration history. At the same time, changes were made to the calibration system itself. Since TRACE-P, the optical configuration has remained fairly constant, so that we have been able to track the calibration history better. As a result, we now have more confidence in the OH and HO_2 measurements from TRACE-P.

Comparison to steady-state box models.

OH and HO_2 were modeled with constrained stead-state box models. Since the measurement suite on the DC-8 included essentially all the known sources, sinks, and reactants with OH and HO_2, the comparison between the observations and the models provides a strong test of the understanding of the HO_x photochemistry. Surprisingly, the observed OH and HO_2 were substantially less than the modeled OH and HO_2 (Figure 5).

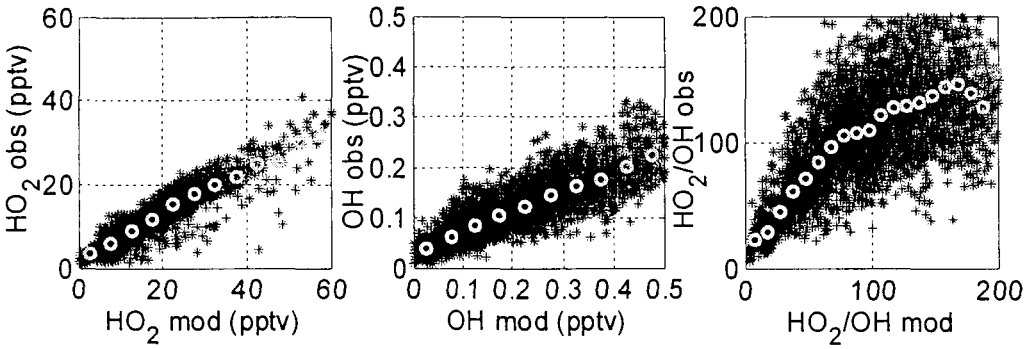

Figure 5. Scatter plots of observed-to-modeled HO_2, OH, and HO_2/OH for TRACE-P.

This difference can also be seen in the statistics, where both the observed-to-modeled ratios and the slope of the a linear fit of observed-to-modeled HO_x are less than 1, with positive intercepts in the case of the linear fits. The mean observed-to-modeled ratio for HO_2 is well within the uncertainty limits of the model and observations; the mean observed-to-modeled OH is closer to the 2σ confidence limits of the combined uncertainty. Note that the correlation coefficients, R^2, are 0.9 or higher for OH and HO_2, while the correlation coefficient for the HO_2/OH ratio is only 0.53.

Table 1. Comparison of observed and modeled HO_x			
	OH	HO_2	HO_2/OH
mean observed/model ratio	0.73	0.79	1.31
median observed/model ratio	0.60	0.75	1.24
slope/intercept: model = slope·observed+int	0.57 / 1.8	0.35 / 0.04	0.42 / 60
R^2 of linear fit	0.94	0.90	0.53

The low correlation in the HO_2/OH ratio appears to result from two effects: the large scatter and the obvious curvature in the relationship between the observed and modeled values. At a ratio of less than ~80, the observed ratio is greater than the modeled ratio, while about 80, the modeled ratio become greater than the observed ratio.

Comparison of observed-to-modeled HO_x as a function of controlling variables.

The observed-to-modeled ratio of OH, HO_2, HO_2/OH and other HO_x parameters can be averaged and plotted as a function of controlling variables in order to examine environmental regimes where observations and models agree and disagree. Further, these quantities can be plotted for SONEX and PEM Tropics B as well as TRACE-P to provide more information about the HO_x chemistry.

For TRACE-P, observed OH is lower than modeled for all altitudes, although the observed-to-modeled ratio is less at higher altitudes, in contrast to what was observed during PEM Tropics B (Figure 6). The observed-to-modeled HO_2 ratio, on the other hand, agrees best at high altitudes, although the observed-to-modeled HO_2 ratio for PEM Tropics B is much closer to 1 than for TRACE-P. The behavior of the ratios for both OH and HO_2 in TRACE-P is much closer to the behavior observed during SONEX than during PEM Tropics B.

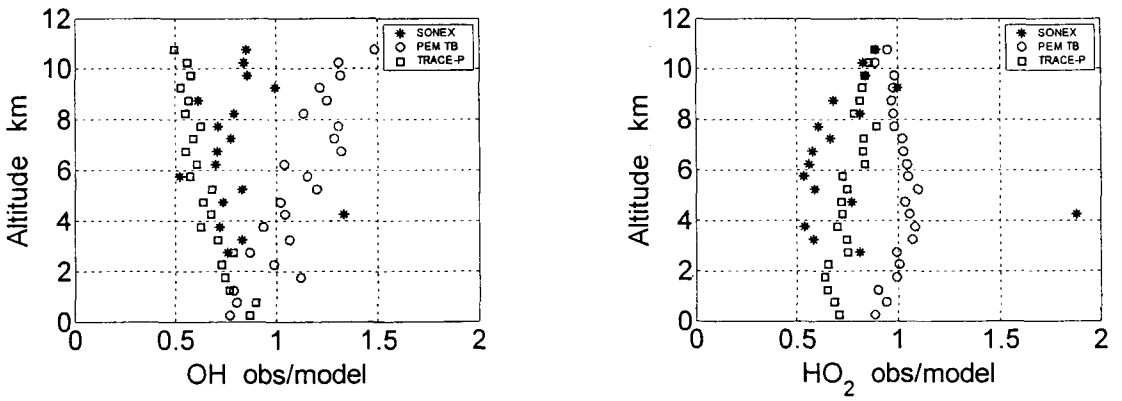

Figure 6. Mean observed-to-modeled HO_x as a function of altitude for TRACE-P, SONEX, and PEM Tropics B. (a) OH and (b) HO_2.

One of the big difference between TRACE-P and PEM Tropics B is the level of pollutants (Figure 7). TRACE-P encountered 2-10 times the NO, 2-4 times the CO, and 2-3 times the O_3 as PEM Tropics B did. The differences in the observed-to-modeled ratios is likely linked to unmeasured pollutants that could be reacting with OH.

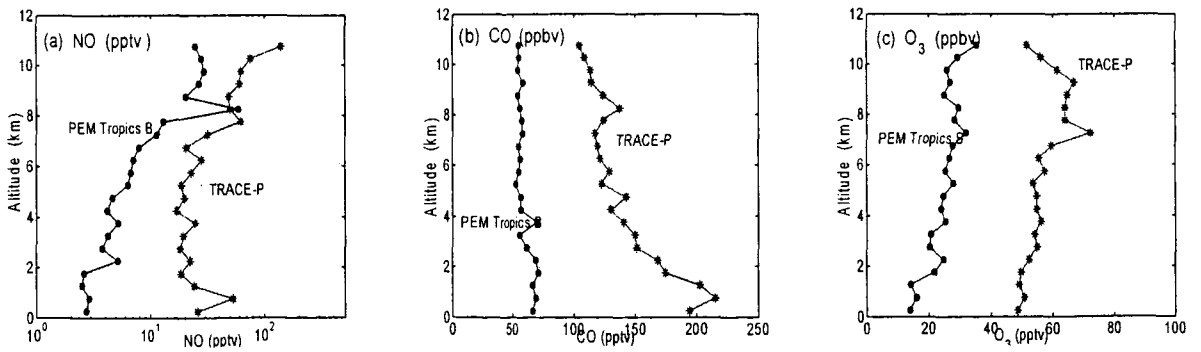

Figure 7. Mean (a) NO, (b) CO, and (c) O_3 as a function of altitude for TRACE-P and PEM Tropics B.

The observed-to-modeled OH and HO_2 have both similarities and differences as a function of NO (Figure 8.)

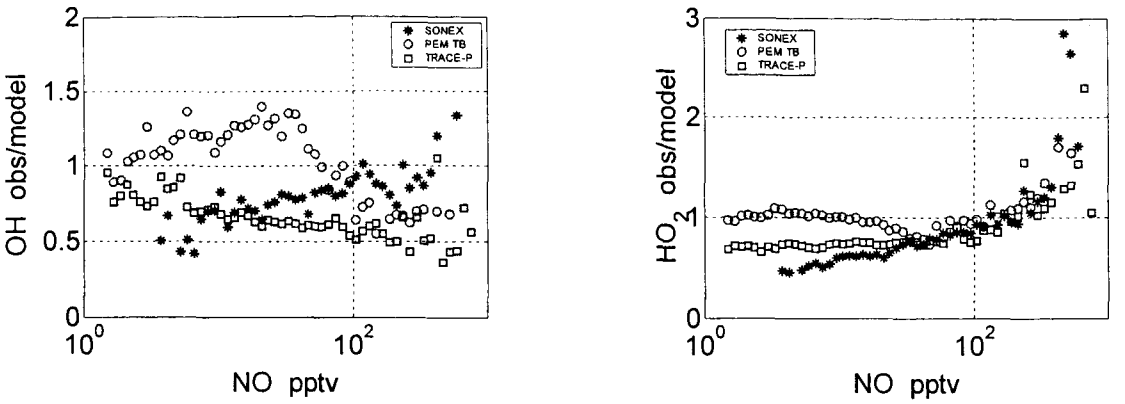

Figure 8. Mean observed-to-modeled HO_x as a function of NO for TRACE-P, SONEX, and PEM Tropics B. (a) OH and (b) HO_2.

The behavior of the observed-to-modeled HO_2 ratio is similar for all three missions for NO > 80 pptv, with deviations of up to a factor of two occurring at the lower NO values. This increase in the observed-to-modeled HO_2 has been observed by us and others for both aircraft and ground-based studies. It is possible that additional unmeasured HO_x sources that increase with increasing NO are the cause, although this behavior is observed for a wide range of HO_x sources and in a wide range of HO_x environments. For OH, the TRACE-P observed-to-modeled ratio is approximately 1 at a few pptv of NO, but then decreases to 0.5 at higher NO. For PEM Tropics B, the observed-to-modeled ratio is greater than 1 at NO below 80 pptv, but decreases to ~0.6 at higher values. Interestingly, all the PEM Tropics B points at NO > 80 pptv come from one segment of one flight, during which that sampled air came recently from a region of convective outflow.

The behavior of the observed-to-modeled OH and HO_2 ratios as a function of $J(O(^1D))$ is similar, even though the absolute ratio is different for PEM Tropics B and TRACE-P and SONEX, which are the same (Figure 9). For OH, the observed-to-modeled ratio decreases monotonically for increasing $J(O(^1D))$, while the observed-to-modeled HO_2 ratio is constant for all but the smallest values. is deviation suggests that whatever is reacting with OH is greatest when the photolytic environment is most intense.

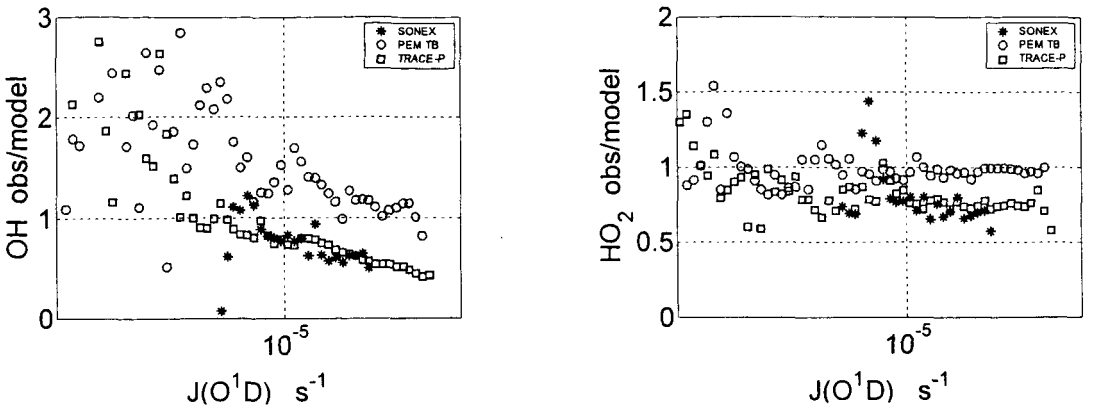

Figure 9. Mean observed-to-modeled HO_x as a function of $J(O^1D)$ for TRACE-P, SONEX, and PEM Tropics B. (a) OH and (b) HO_2.

A last test is the observed-to-modeled ratio of the HO_2/OH ratio (Figure 10). When plotted as a function of NO, the observed-to-modeled ratio agrees for very low NO values, but increases to greater than 2 when NO exceeds 100 pptv. The mean values for SONEX and PEM Tropics are in good agreement for the entire range of NO encountered, and close to 1 for NO < 100 pptv. The mean observed-to-modeled ratio for TRACE-P becomes greater than 1 at about 10 pptv of NO, and is larger than the ratios from either PEM Tropics B or SONEX for all values of NO larger than 10 pptv. At very low values of NO, O_3 controls the cycling from HO_2 to OH, while at larger values of NO, NO does.

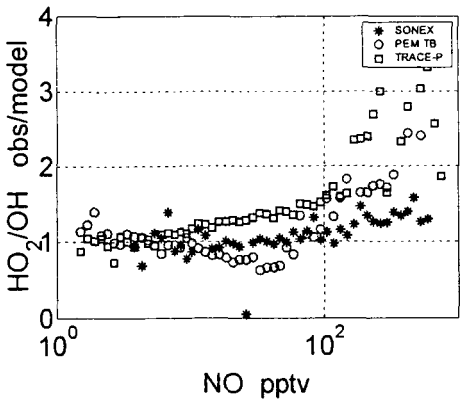

Figure 10. Mean observed-to-modeled HO_x/OH as a function of NO for TRACE-P, SONEX, and PEM Tropics B.

This behavior suggests that the cycling between OH and HO_2 is well understood in the clean conditions represented by low NO when O_3 is in control of the cycling of HO_2 to OH. However, the cycling from HO_2 to OH at higher values of NO is controlled by NO. These measurements suggest that the Asian outflow contains unmeasured chemicals that are reacting with OH. If this is the case, then the reactivity of unmeasured reactant is greatest at the highest altitudes and the highest photolytic activity. It should be noted that small amounts of reactive halogens – a few pptv of BrO, for instance, can dramatically influence the HO_2/OH ratio. Is it possible that tropospheric reactive halogens are

influencing the HO_x photochemistry? Or is the supposed additional reactant related to VOC oxidation? These questions need to be answered.

Net ozone production.

The net ozone production can be found from the equation:

$$\frac{d[O_3]}{dt} = \left(k_{HO2+NO}[NO][HO_2] + \sum k_{RO2i+NO}[NO][RO_{2i}]\right) - \left(J(O(^1D))f[O_3] + k_{O3+HO2}[O_3][HO_2] + k_{O3+OH}[O_3][OH]\right)$$

where k are the reaction rate coefficients, J is the photolysis frequency, and f is the fraction of $O(^1D)$ molecules that react with water vapor.

The concentrations of RO_{2i} are unknown. Only the net production due to HO_2 is considered. If we assume that $[RO_2] \sim [HO_2]$, then the total ozone production will be about twice that for HO_2 at higher values of NO and the NO concentration at which $P(O_3)$ goes from being negative to positive would be greater than the 30-40 pptv that is both observed and modeled.

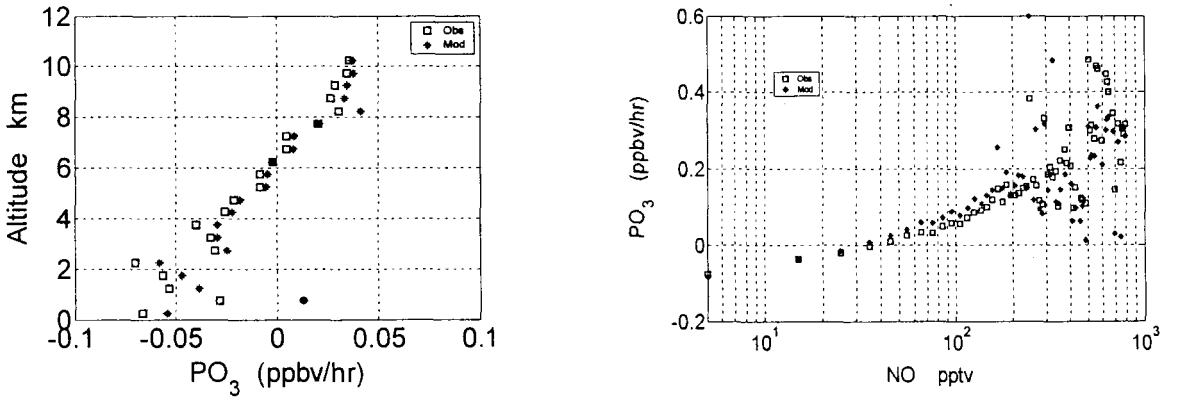

Figure 11. Mean net ozone production from HO_2 as a function of altitude (left) and NO (right). Red starts are modeled $P(O_3)$ and blue squares are observed $P(O_3)$.

Mean net chemical ozone production is negative below 6 km altitude and becomes positive only above 6 km. In the mean, $P(O_3)$ is less than 0.05 ppbv/hr, both as a loss below 6 km and a gain above 6 km. On the other hand, $P(O_3)$ is as high as 0.2-0.4 ppbv/hr in air masses that contain a few hundred pptv of NO. The net ozone production derived from modeled and observed HO_2 shows no evidence of reaching its peak value for NO as great as 800 pptv, although a more careful analysis that averages the data in bins of constant HO_x production may be necessary to be sure.

Examining the proposed hypotheses.

What can be said about the proposed hypotheses? Each is repeated and then discussed.

Asian outflow contains a unique mixture of HO_x sources; these, in combination with outflow and lightning NO_x, can shift large regions of the Pacific troposphere from being ozone-destroying toward being ozone producing.

We have not done enough analysis at this time to answer this question. However, by comparing observed and modeled HO_x, it appears that the more polluted air encountered during TRACE-P contains unmeasured reactants with OH, thus reducing, not increasing, HO_x in these plumes.

As Asian outflow mixes with cleaner Pacific air, ozone production that is calculated from HO_2 and NO measurements is greater than that calculated by chemical transport models;

It does not appear that ozone production that is calculated for HO_2 and NO measurements is significantly different from that calculated by chemical transport models.

Atmospheric oxidation over the western tropical Pacific is affected by the evolution of Asian outflow, but whether it is increased or decreased depends on the composition of the outflow and the influence of convection on that composition.

Testing this hypothesis will require more analysis.

Asian aerosols influence HO_x and atmospheric oxidation; they must be considered when calculating the influence of the Asian outflow on the photochemistry of the Pacific troposphere.

While Asian aerosols may affect the photolysis frequencies, and while Cantrell et al. found evidence of HO_2+RO_2 reduction in the presence of aerosols, we have not done the analysis in the same manner they employed to determine if we get the same effect. This effort is underway now.

The outflow of HO_x sources into the Pacific free troposphere has greater influence on increasing ozone production than does the NO_x outflow because of the greater horizontal range of HO_x sources compared to that of NO_x and the availability of NO_x from lightning.

An analysis of this issue will be included in the manuscript in preparation.

In summary, more analysis needs to be done to resolve these hypotheses. However, we have been successful in defining the behavior of HO_x in the Asian pollution plumes and are proceeding with the necessary analyses.

Publications

W. H. Brune, H. Harder, M. Martinez, J. Crawford, J. Olson, The behavior of OH and HO_2 during TRACE-P: Comparison with their behavior during PEM Tropics B and SONEX, in preparation.

Edward V. Browell, Marta A. Fenn, Carolyn F. Butler, William B. Grant, Vincent G. Brackett, Johnathan W. Hair, Melody A. Avery, Reginald E. Newell, Yuanlong Hu, Henry E. Fuelberg, Daniel J. Jacob, Bruce E. Anderson, Elliot L. Atlas, Donald R. Blake, William H. Brune, Jack E. Dibb, Alan Fried, Brian G. Heikes, Glen W. Sachse, Scott T. Sandholm, Hanwant B. Singh, Robert W. Talbot, Stephanie A. Vay, Rodney J. Weber, and Karen B. Bartlett, Large-scale ozone and aerosol distributions, air mass characteristics, and ozone fluxes over the western Pacific Ocean in late winter/early spring, J. Geop[hys. Res., 108, D20, 8805, doi:10.1029/2002JD003290, 2003

Christopher A. Cantrell, G. D. Edwards, S. Stephens, R. L. Mauldin, M. A. Zondlo, E. Kosciuch, F. L. Eisele, R. E. Shetter, B. L. Lefer, S. Hall, F. Flocke, A. Weinheimer, A. Fried, E. Apel, Y. Kondo, D. R. Blake, N. J. Blake, I. J. Simpson, A. R. Bandy, D. C. Thornton, B. G. Heikes, H. B. Singh, W. H. Brune, H. Harder, M. Martinez, D. J. Jacob, M. A. Avery, J. D. Barrick, G. W. Sachse, J. R. Olson, J. H. Crawford, and A. D. Clarke, Peroxy radical behavior during the Transport and Chemical Evolution over the Pacific (TRACE-P) campaign as measured aboard the NASA P-3B aircraft, J. Geophys. Res., 108, D20, 8797, doi:10.1029/2003JD003674, 2003

G. R. Carmichael, Y. Tang, G. Kurata, I. Uno, D. Streets, J.-H. Woo, H. Huang, J. Yienger, B. Lefer, R. Shetter, D. Blake, E. Atlas, A. Fried, E. Apel, F. Eisele, C. Cantrell, M. Avery, J. Barrick, G. Sachse, W. Brune, S. Sandholm, Y. Kondo, H. Singh, R. Talbot, A. Bandy, D. Thorton, A. Clarke, and B. Heikes, Regional-scale chemical transport modeling in support of the analysis of observations obtained during the TRACE-P Experiment, J. Geophys. Res., 108, D21, 8823, doi:10.1029/2002JD003117, 2003

J. Crawford, J. Olson, D. Davis, G. Chen, J. Barrick, R. Shetter, B. Lefer, C. Jordan, B. Anderson, A. Clarke, G. Sachse, D. Blake, H. Singh, S. Sandolm, D. Tan, Y. Kondo, M. Avery, F. Flocke, F. Eisele, L. Mauldin, M. Zondlo, W. Brune, H. Harder, M. Martinez, R. Talbot, A. Bandy, and D. Thornton, Clouds and trace gas distributions during TRACE-P, J. Geophys. Res., 108, D21, 8818, doi:10.1029/2002JD003177, 2003

F. L. Eisele, L. Mauldin, C. Cantrell, M. Zondlo, E. Apel, A. Fried, J. Walega, R. Shetter, B. Lefer,1 F. Flocke, A. Weinheimer, M. Avery, S. Vay, G. Sachse, J. Podolske, G. Diskin, J. D. Barrick, H. B. Singh, W. Brune, H. Harder, M. Martinez, A. Bandy, D. Thornton, B. Heikes, Y. Kondo, D. Riemer, S. Sandholm, D. Tan, R. Talbot, and Jack Dibb, Summary of measurement intercomparisons during TRACE-P, J. Geophys. Res., 108, D20, 8791, doi:10.1029/2002JD003167, 2003